

Understanding vitrification during cure of epoxy resins using dynamic scanning calorimetry and rheological techniques

J. Lange¹, N. Altmann, C.T. Kelly, P.J. Halley*

Department of Chemical Engineering, MCP Centre, The University of Queensland, Brisbane, QLD 4072, Australia

Received 27 August 1999; accepted 14 October 1999

Abstract

The gelation and vitrification transitions during cure of an epoxy-amine system are examined using rheological, modulated differential scanning calorimetry (DSC) and FTIR techniques. The results from dynamic mechanical analysis show that gelation is observed before vitrification at all temperatures where it can be rheologically defined. By comparing different rheological criteria for vitrification, it is seen that the vitrification transition is a gradual process that extends over a large part of cure at all temperatures where it occurs. Results from modulated DSC measurements show that the calorimetric vitrification times are longer than the vitrification times obtained from rheological measurements at cure temperatures above 100°C, but that at lower temperatures calorimetric vitrification occurs before, or at the same time as, rheological vitrification. Theoretical gelation times, estimated from FTIR conversion data, were found to be consistently shorter than the observed gelation times. Theoretical vitrification times agreed well with the observed times. The magnitude of the vitrification transition, expressed either as amount of change in heat capacity or as maximum value of loss tangent, was found to decrease approximately linearly with increasing cure temperature. © 2000 Elsevier Science Ltd. All rights reserved.

Keywords: Gelation and vitrification transitions; Modulated differential scanning calorimetry; Time–temperature transformation diagram

1. Introduction

For thermosetting materials such as amine cured epoxy resins, the solidification behavior during cure both defines the processing window and determines the properties of the final material. Substantial efforts have been devoted to developing the techniques required for characterizing the solidification transitions [1–5] as well as to investigating the behavior of different systems [1,4,6–8]. However, in spite of the large number of studies reported in the literature, some issues, such as the nature and detection of the vitrification transition, merit further attention [5].

The two main events that occur during the crosslinking polymerization reaction of thermosets are gelation, i.e. liquid-to-rubber transition, and vitrification, i.e. liquid or rubber-to-glass transition. Gelation is a well-characterized, distinct and non-reversible event which occurs at a certain degree of conversion. Gelation is often detected using rheological techniques [2,4,8–12], but a number of other

techniques have been proposed [8,13–15]. Vitrification is a gradual, thermo-reversible process, and its detection will vary with the technique employed. Although several methods are available for characterizing the behavior of non-reacting systems at the glass transition, only a few techniques are capable of directly quantifying isothermal vitrification during cure. Therefore, in many studies vitrification is only detected indirectly, through temperature scans on partially cured samples [6]. Most of the work reported so far on isothermal determination of vitrification has been on changes in dynamic mechanical properties [16–18], but also chemiluminescence [18] and dielectric techniques [19,20] have been employed. Recently it has been shown that the modulated density scanning calorimetry (MDSC), which provides quasi-isothermal measurement of the heat capacity C_p , can be used to follow the vitrification process [21–25]. Results indicating qualitative agreement between dynamic mechanical and MDSC vitrification data have been presented [24,25].

The sequence of events the reacting system will undergo depends on the cure temperature (T_{cure}). According to the majority of the studies undertaken, the same behavior is observed in all systems [1]. Thus, when T_{cure} is above the ultimate glass transition temperature ($T_{g\infty}$) of the cured

* Corresponding author. Tel.: +61-7-3365-4158; fax: +61-7-3365-4199.

E-mail address: p.halley@cheque.uq.edu.au (P.J. Halley).

¹ Present address: Nestlé Research Center, Vers-chez-les-Blanc, CH-1000 Lausanne 26, Switzerland.

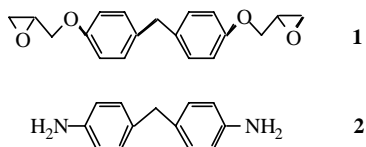


Fig. 1. Epoxy (**1**) and amine (**2**) monomers.

material, the system will only gel. If T_{cure} is below $T_{\text{g}\infty}$ but above the glass transition temperature of the material at the gel point ($_{\text{gel}}T_{\text{g}}$), the system will first gel and then vitrify. Finally, when T_{cure} is below $_{\text{gel}}T_{\text{g}}$ the system will first vitrify and then, if given enough time, undergo gelation. In many systems the mobility in the vitrified state is too low to permit further reaction, in which case only vitrification occurs. However, some studies have reported results that do not agree with this general picture. Gelation has been found to occur before vitrification at all cure temperatures where it could be observed, i.e. also below $_{\text{gel}}T_{\text{g}}$ [4].

In order to visualize how the sequence of events varies with cure temperature, time–temperature–transformation (TTT) diagrams, presenting the times to gelation and vitrification as a function of cure temperature, have been developed [1,6–8]. TTT diagrams have been established for a wide variety of different systems, and are useful as a basis for designing and modifying the time–temperature program for thermoset processing. Often the TTT diagrams are constructed not from direct experimental observation of gelation and vitrification during isothermal cure, but from time-conversion data generated by kinetic models together with knowledge of gel point conversion and of the T_{g} -conversion relationship. Whereas this modeling approach is convenient and paves the way for modeling of the entire cure process, it does not permit as detailed an examination of the transitions as the direct experimental approach. Few studies examining TTT data obtained through detailed experimental investigation of isothermal vitrification have been presented.

In the present work the gelation and vitrification transitions during cure of an epoxy-amine system are examined using rheological and modulated DSC techniques. The relation between vitrification detected through changes in dynamic modulus and through changes in heat capacity is investigated. Detailed TTT diagrams are presented, and the influence on the diagram of how vitrification is determined is discussed. In this way, it is anticipated that a better understanding of the vitrification process may be gained.

Table 1
Properties of the epoxy-amine system

Property	Value
$T_{\text{g}0}$	– 20°C
$T_{\text{g}\infty}$	150°C
Rubbery modulus	10 MPa
Glassy modulus	2600 MPa

2. Experimental

2.1. Materials

The diglycidyl ether of Bisphenol F (**1**) was received from Ciba Specialty Chemicals, Australia. 4,4'-Diaminodiphenylmethane (**2**) was obtained from Aldrich. All chemicals were used without further purification. The monomers are presented in Fig. 1.

2.2. Methods

Dynamic mechanical analysis was performed in a Rheometrics RDS 2, using parallel plates of 8 mm diameter and samples of approximately 4 mm diameter and 1.5 mm thickness. The samples, stoichiometric mixtures of **1** and **2**, were placed in the instrument at ambient temperature, and brought to the cure temperature at 15°C/min. The complex modulus was measured at regular intervals throughout the heating up and cure process using a multi-wave technique involving superposition and decomposition of the signal, which permitted data at several frequencies to be collected simultaneously. The strain was 0.3% and the frequencies 0.2, 1 and 5 Hz. Initial work was conducted to ensure that the response was in the linear viscoelastic region. The sample dimensions were checked after cure, and the real sample dimensions used to convert the instrument signal into modulus data.

Modulated DSC measurements were run on a TA Instruments 2920 DSC. Samples of about 10 mg were placed in the instrument at ambient temperature and brought to the cure temperature at 15°C/min. The heat capacity was measured at regular intervals throughout the cure process using a continuous temperature modulation of $\pm 0.1^\circ\text{C}$ with a period of 60 s. In another series of experiments, samples were cured isothermally for different times after which the sample was cooled at 20°C/min and the T_{g} determined by a scan at 5°C/min.

FTIR measurements were performed using a Perkin Elmer System 2000 FTIR Spectrometer. Samples were cured in an oven inside the spectrometer and the conversion measured by following the change in intensity of the epoxide band at 4530 cm^{-1} [26].

The gel content of the rheometer samples was measured by solvent extraction in dichloromethane. A Branson Sonifier 450 ultrasonic probe was used to accelerate the extraction. The samples were weighed, immersed in solvent for 24 h, extracted ultrasonically for 10 min, dried under vacuum and then weighed again.

3. Results and discussion

The properties of the investigated epoxy-amine system are presented in Table 1. Cure tests were performed at temperatures between 40 and 170°C.

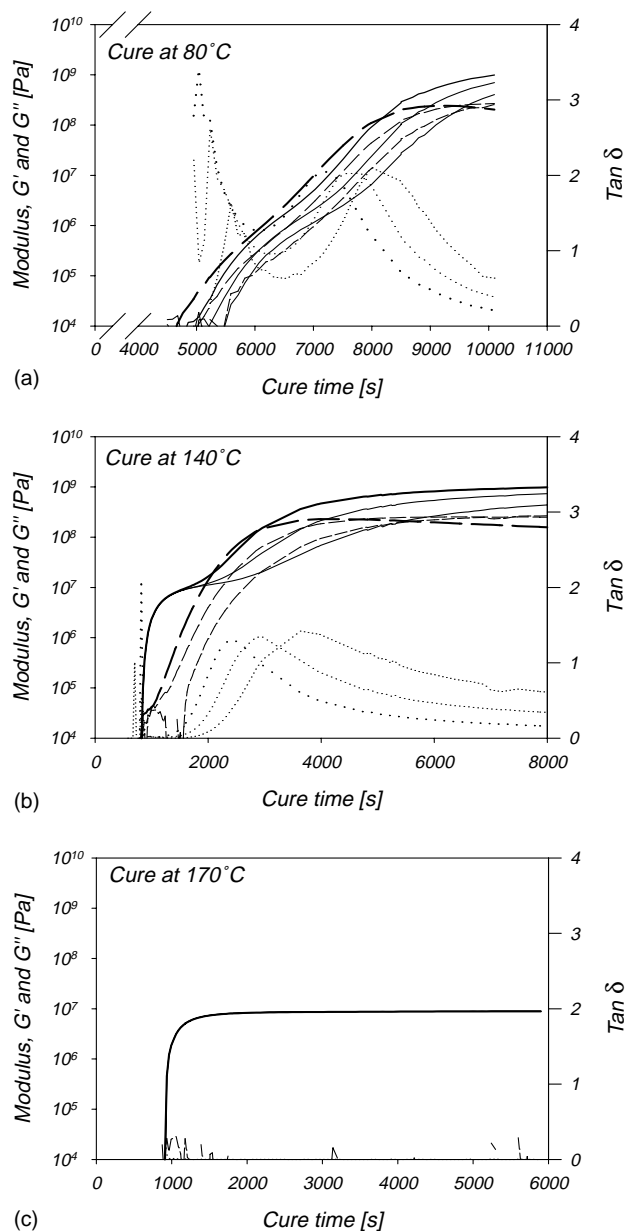


Fig. 2. G' (solid lines), G'' (dashed lines) and $\tan \delta$ (dotted lines) measured at 0.2 Hz (fine lines), 1 Hz (medium lines) and 5 Hz (heavy lines) during cure at different temperatures.

Table 2
Criteria for detection of gelation and vitrification

Criterion	Definition
Gelation	$\tan \delta$ independent of frequency
Vitrification 1	Onset of frequency dependence in G'
Vitrification 2	Peak in $\tan \delta$ at 1 Hz
Vitrification 3	Peak in G'' at 1 Hz
Vitrification 4	End of frequency dependence in G'
Vitrification 5	Onset of change in C_p
Vitrification 6	End of change in C_p

3.1. Rheological characterization

As mentioned above, gelation and vitrification during isothermal cure can be detected through changes in the dynamic mechanical properties. Extensive work on gelation has established that it is most precisely detected as the point at which the loss tangent, $\tan \delta$, becomes independent of measurement frequency [2,27]. For vitrification no generally accepted criterion has been defined [17,18]. It should be noted that it is difficult with dynamic mechanical analysis to accurately measure properties through the whole cure process (liquid–gel–glass) using one single geometry, since the stiffness typically changes seven orders of magnitude. In the present work the geometry was chosen to give reliable data in the part of the process following gelation, which means that the readings before and during gelation show significant scatter. The evolution of the elastic modulus, G' , the loss modulus, G'' , and $\tan \delta$ at three frequencies during cure of the epoxy-amine mixture at different temperatures is depicted in Fig. 2. Initially the same behavior is observed at all temperatures. Before gelation the system is liquid, and the stiffness too low to be detected. As the sample then gels there is a rapid increase in stiffness, and G' becomes independent of frequency except at the lowest cure temperature. From this point onwards the behavior depends on the cure temperature. At temperatures below T_g^∞ , i.e. 80 and 140°C, the system vitrifies, as indicated by the continuing rise in G' , G'' and $\tan \delta$, beginning at high frequencies, and the onset of frequency dependence of G' . At 80°C vitrification goes to completion, as evidenced by the decrease in $\tan \delta$ and G'' and decrease in frequency dependence of G' towards the end of cure. On cure close to T_g^∞ (140°C), vitrification is no longer complete and the sample is still in the transition zone at the end of cure. At temperatures above T_g^∞ , i.e. 170°C, only gelation is observed; $\tan \delta$ and G'' remain low and there is no frequency dependence in G' .

By applying criteria for gelation and vitrification to the dynamic-mechanical data, and plotting the corresponding times versus cure temperature, a TTT diagram can be constructed [8]. In the present work, one criterion for gelation and four criteria for vitrification were applied to the dynamic-mechanical data. The criteria selected were $\tan \delta$ crossover (independence of measurement frequency) for gelation [2], and (1) onset of frequency dependence in G' , (2) peak in $\tan \delta$ at 1 Hz, (3) peak in G'' at 1 Hz for vitrification and (4) end of frequency dependence in G' [17,18,29]. The emergence of a frequency-dependence in G' can be taken as a sign of vitrification only as long as vitrification is preceded by gelation [18,28]. For the present system, this was found to be valid down to a cure temperature of 100°C. Furthermore, it should be noted that as vitrification occurs closer and closer to gelation, it becomes difficult to observe the gel point. For the present epoxy-amine system, it was not possible to define a rheological gel point below a cure temperature of 80°C. The gelation

Table 3
Gelation and vitrification times (s) (nd, not detectable)

Cure temp. (°C)	Gelation	Vitrification 1 (ons. Freq. dep. G')	Vitrification 2 (peak $\tan \delta$)	Vitrification 3 (peak G'')	Vitrification 4 (end freq. dep. G')	Vitrification 5 (ons. C_p)	Vitrification 6 (end C_p)	Theoretical gelation	Start theoretical vitrification	End theoretical vitrification
40	nd	nd	nd	50000 ± 1000	60000 ± 1000			19 300	18 000	25 000
50	nd	nd	nd	28000 ± 1000	33000 ± 1000			9000	11 000	18 000
60	nd	15000 ± 1000	9600 ± 500	17100 ± 1000	204000 ± 1000	12600 ± 700	16000 ± 700	6800	8900	13 000
70	nd	9600 ± 500	6900 ± 500	11500 ± 600	13000 ± 700	6000 ± 400	7800 ± 400	4100	5000	7700
80	5200 ± 300	nd	5100 ± 300	7800 ± 300	9200 ± 500	3400 ± 300	4500 ± 300	3100	3900	6300
90	3500 ± 300	nd	3700 ± 200	5900 ± 300	6900 ± 300	2500 ± 300	3600 ± 300	2100	3200	5200
100	2400 ± 300	2900 ± 300	2900 ± 200	4400 ± 200	5600 ± 300	3000 ± 500	~ 9000	1400	2100	3800
110	1600 ± 200	2100 ± 300	2500 ± 200	3400 ± 200	4800 ± 200	nd	nd	1100	1700	4400
120	1300 ± 100	1700 ± 200	2300 ± 200	3100 ± 200	4500 ± 200	nd	nd	900		
130	1000 ± 100	1500 ± 200	2600 ± 200	3100 ± 200	5100 ± 200	nd	nd			
140	800 ± 100	1400 ± 200	nd	nd	nd	nd	nd			
150	800 ± 100	1900 ± 200	nd	nd	nd	nd	nd			
170	800 ± 100	nd	nd	nd	nd	nd	nd			

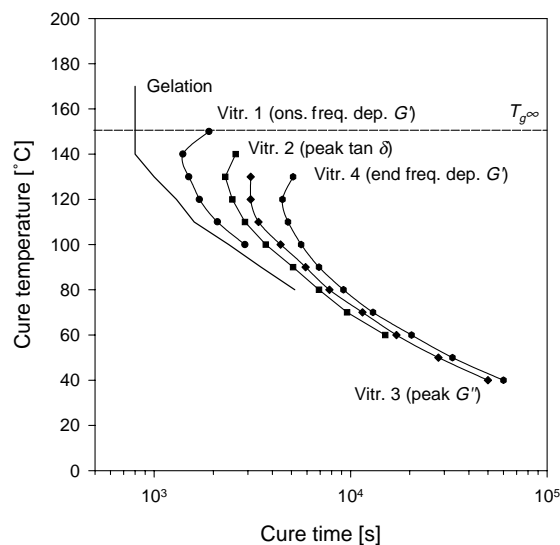


Fig. 3. Times to gelation and vitrification from dynamic mechanical measurements. The gelation and vitrification criteria are defined in Table 2.

and vitrification criteria are summarized in Table 2. The rheological gel- and vitrification times obtained for the epoxy-amine system are presented in Table 3 and Fig. 3. As can be expected, the gel times increase with decreasing cure temperatures, whereas the vitrification times show the characteristic minimum at intermediate cure temperatures [1]. It is also evident that vitrification is a process that extends over a large part of the cure.

3.2. Heat capacity

Fig. 4 shows the evolution of the C_p during cure of the epoxy-amine mixtures at different temperatures. On cure at 80°C a step change in C_p is observed, indicating that the sample fully vitrifies during cure. Cure at 140°C, i.e. close to T_g , produces the beginning of a transition but at the end of cure (as defined by the time to reach constant conversion in FTIR measurements), C_p has not yet reached a stable value. The dynamic-mechanical data indicated that vitrification does not proceed to completion at this temperature. However, while the dynamic-mechanical properties appear fairly stable at the end of cure, this is not the case for C_p . When cured above T_g , i.e. at 170°C, no change in C_p is observed.

The vitrification times as determined by the times to onset and end of the C_p change are presented in Table 3 and together with the gelation and vitrification times from the dynamic-mechanical data in Fig. 5. It can be seen that vitrification in terms of C_p in general follows the rheological vitrification data. However, at cure temperatures above 100°C vitrification is detected somewhat later in terms of C_p than in rheological terms. Previous non-isothermal work comparing calorimetric and dynamic mechanical determination of vitrification has shown that the peak in G'' is the measure that correlates best with C_p change [29,30]. In general, vitrification is detected at somewhat lower

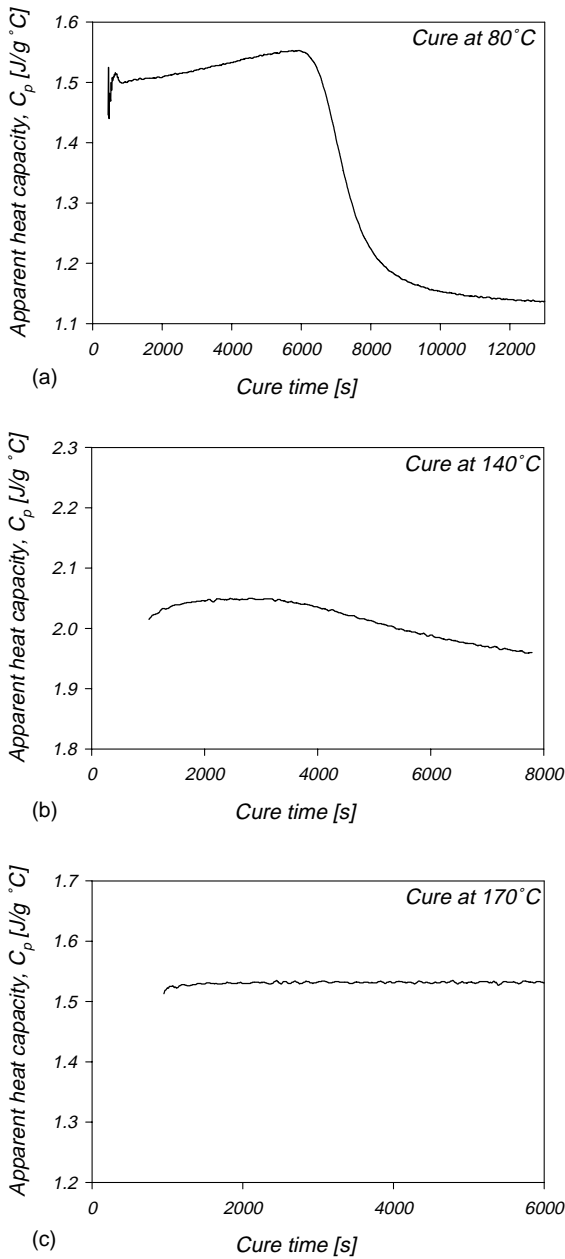


Fig. 4. Heat capacity as a function of time during isothermal cure at different temperatures.

temperatures by calorimetry than by dynamic mechanical analysis [29], which means that isothermal vitrification should be detected later in terms of C_p than in terms of dynamic mechanical properties. Thus, the expected behavior is observed at temperatures above 100°C. Why this is not the case at cure temperatures below 100°C is not fully understood.

3.3. Conversion

Fig. 6 presents the relationship between T_g and conversion for the epoxy-amine system. The curve was obtained by combining data on T_g as a function of cure

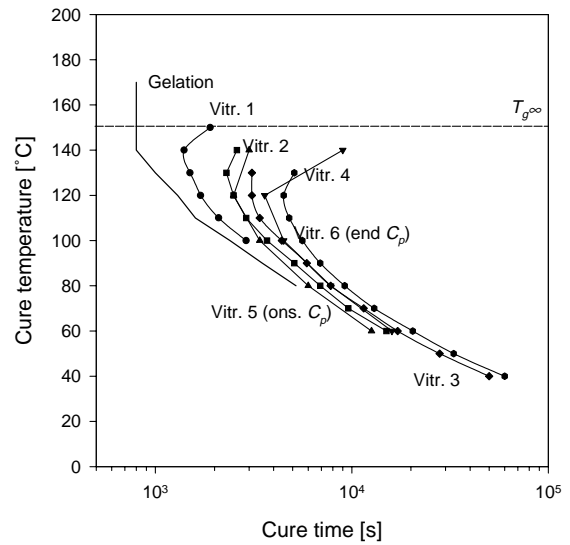


Fig. 5. Times to gelation and vitrification from dynamic mechanical measurements and modulated DSC measurements. The gelation and vitrification criteria are defined in Table 2.

time from DSC with conversion vs. cure time data from FTIR. The gel point conversion for a 2 + 4-functional system such as the present epoxy-amine system is 0.6 [5,31], which, allowing for some scatter, gives $_{gel}T_g$ of 20–40°C. Fig. 6 also shows the gel fraction of samples cured at different temperatures. It can be seen that cure at 20°C results in a sizable gel fraction, in spite of the fact that this temperature is below, or at the limit of, the $_{gel}T_g$. It thus appears that the reaction progresses significantly also after the T_g of the curing system has reached the cure temperature.

Estimates of the conversions at which vitrification begins and ends at each cure temperature can be obtained by

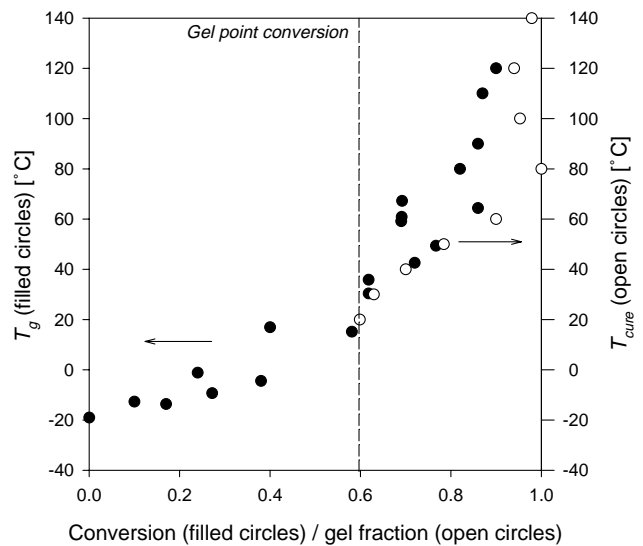


Fig. 6. Conversion versus glass transition temperature (filled circles) and gel fraction versus cure temperature (open circles).

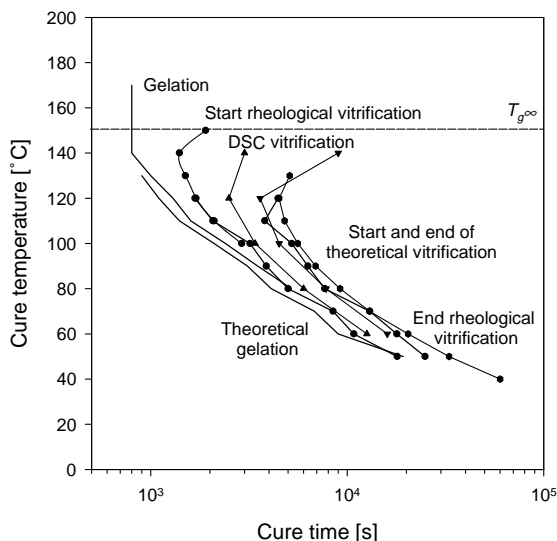


Fig. 7. Theoretical times to gelation (line) and vitrification (start: open circles, end: filled circles) together with times to gelation and vitrification from dynamic mechanical analysis and modulated DSC (gray lines). The gelation and vitrification criteria are defined in Table 2.

extracting the maximum and minimum conversions for $T_g = T_{\text{cure}}$ from Fig. 6. Using FTIR conversion–cure time data it is then possible to convert these vitrification conversions as well as the gel point conversions into theoretical gelation and vitrification times. In Fig. 7 such theoretical times are shown together with observed gelation and vitrification times. It can be seen that gelation is generally detected somewhat later than predicted, which is in accordance with previous observations [4,8,11]. For vitrification, it can be seen that the correlation between theory and observation is quite good. A detailed examination of the start of vitrification (see also the data in Table 3) reveals that the prediction correlates with the earliest observations at all temperatures, i.e. with the rheological vitrification observations

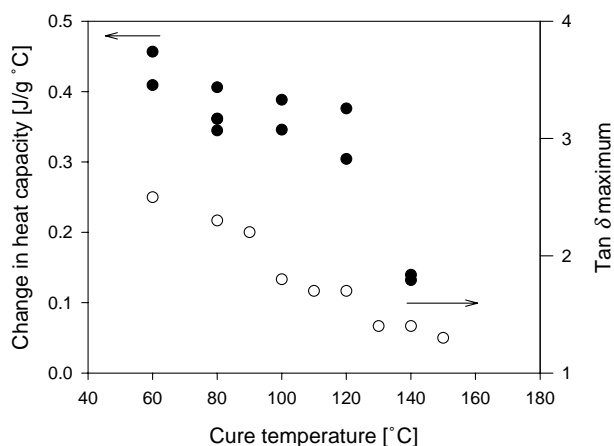


Fig. 8. Intensity of the glass transition, expressed as change in heat capacity on vitrification (filled circles) and maximum value of loss tangent (open circles) during vitrification, as a function of isothermal cure temperature.

at temperatures above 90°C and with the calorimetric observations at lower temperatures.

3.4. Magnitude of the vitrification transition

The intensity or magnitude of the vitrification transition depends on the difference in mobility between the rubbery and the glassy state [28,32]. In calorimetric determination of vitrification, the amount of change in C_p can be used as a measure of the magnitude of the transition [32]. For dynamic mechanical analysis the peak value of, or area under, the $\tan \delta$ curve provides the same information [30,33]. Fig. 8 shows data on the C_p change and peak value of $\tan \delta$ on vitrification as a function of cure temperature. It can be seen that the intensity of the vitrification transition decreases with increasing cure temperature. Since the crosslink density increase as the reaction proceeds and vitrification will occur at progressively higher degrees of conversion as the cure temperature is increased, a decrease in transition intensity with increasing cure temperature is expected [34]. It can be seen for both parameters that the variation with cure temperature is approximately linear, except for the DSC data at the highest cure temperature. The deviation at this point is believed to be due to the previously mentioned fact that the C_p does not reach its equilibrium value during the experiment time.

3.5. Gel and vitrification time crossover

One of the main observations in the area of thermoset cure made by Gillham and others is the presence of a $_{\text{gel}}T_g$ below which cure will only lead to vitrification, gelation being inhibited by the low rate of reaction in the glassy state [1,6]. As a consequence, experimental observations of gelation and vitrification are expected to show gel and vitrification times that move closer and closer as the cure temperature is decreased until $_{\text{gel}}T_g$ is reached, where the gel point should disappear. However, all experimental observations show gelation to take place before vitrification, also at cure temperatures below the designated $_{\text{gel}}T_g$ [4,8]. Furthermore, although the curves appear to grow closer in a log plot, the actual time lag between the transitions is seen to gradually increase as the cure temperature is lowered [4]. Therefore, some authors have argued that the fact that gelation no longer is observed below a certain cure temperature is not related to vitrification [4]. In the present study, the experimentally observed gel- and vitrification times also exhibit an ever increasing time lag with decreasing cure temperature down to the temperature where gelation no longer is definable (see Table 3). However, the same does not hold for the theoretical gel- and vitrification times where the time lag decreases at the lowest examined temperature, and a crossover indeed can be observed at about 50°C. This is at the high end of the estimated $_{\text{gel}}T_g$ range of 10–40°C, which is related to the fact that the crossover is between the start of vitrification and gelation. The fact that a gel fraction is found in samples cured at 20°C also shows that gelation

occurs at temperatures well below the temperature at which the rheological signs of gelation disappear. To conclude, it appears that the disappearance of gelation is an artifact related to the rheological detection criterion employed rather than a characteristic of the cure process.

4. Conclusions

The transitions during isothermal cure of an epoxy-amine system have been investigated. Dynamic mechanical analysis shows that gelation is observed before vitrification at all temperatures where it can be rheologically defined. It is seen that the vitrification transition is a gradual process that extends over a large part of cure at all temperatures where it occurs.

In modulated scanning calorimetry measurements, the vitrification transition is observed as a step change in heat capacity. According to previous non-isothermal work, the calorimetric vitrification times are expected to be somewhat longer than the vitrification times obtained from rheological measurements. The expected behavior is observed at cure temperatures above 100°C, but at lower temperatures calorimetric vitrification occurs before, or at the same time as, rheological vitrification.

Gel fraction measurements show that the cure reaction proceeds well beyond gelation also at cure temperatures just below $_{gel}T_g$. In agreement with previous results, theoretical gel times obtained from FTIR measurements were found to be overall slightly shorter than observed times to gelation. Theoretical vitrification times were seen to agree well with rheological and calorimetric vitrification observations.

The magnitude of the vitrification transition expressed either as amount of change in heat capacity or as maximum value of loss tangent, is found to decrease approximately linearly with increasing cure temperature.

Acknowledgements

Financial support from the Wennergren Foundation and the Australian Research Council is gratefully acknowledged.

References

- [1] Gillham JK, Enns JB. Trends Polym Sci 1994;2:406.
- [2] Winter HH. Polym Eng Sci 1987;27:1698.
- [3] Halley PJ, Mackay ME. Polym Eng Sci 1996;36:593.
- [4] Harran D, Laudouard A. J Appl Polym Sci 1986;32:6043.
- [5] Lange J, Hult A, Månson J-AE. Polymer 1996;37:5859.
- [6] Barral L, Cano J, Lopez AJ, Lopez J, Nogueira P, Ramirez C. Polym Int 1995;38:353.
- [7] Barral L, Cano J, Lopez J, Nogueira P, Ramirez C, Abad MJ. Polym Int 1997;42:301.
- [8] Gillham JK, Enns JB. J Appl Polym Sci 1983;28:2567.
- [9] Malkin AYa, Kulichikin SG. Adv Polym Sci 1991;101:218.
- [10] Halley PJ, Mackay ME, George GA. High Perform Polym 1994;6:405.
- [11] Matejka L. Polym Bull 1991;26:109.
- [12] Farris RJ, Lee CJ. Polym Eng Sci 1983;23:586.
- [13] Senturia SD, Sheppard NF. Adv Polym Sci 1986;80:3.
- [14] George GA. Mater Forum 1986;9:224.
- [15] George GA, Schweinsberg DP. J Appl Polym Sci 1987;33:2281.
- [16] Hofmann K, Glasser WG. Thermochim Acta 1990;166:169.
- [17] Lange J. Polym Engng Sci 1999;39:1651.
- [18] Lange J, Ekelöf R, George GA. Polymer 1998;40:149.
- [19] Casalini R, Corezzi S, Fioretti D, Livi A, Rolla PA. Chem Phys Lett 1996;258:470.
- [20] Chow AW, Bellin JL. Polym Engng Sci 1992;32:182.
- [21] Gill P, Sauerbrunn S, Reading M. J Thermal Anal 1993;40:931.
- [22] Cassettari M, Salvetti G, Tombari E, Veronesi S, Johari GP. J Polym Sci, Polym Phys Ed 1993;31:199.
- [23] Van Assche G, Van Hemelrijk A, Rahier H, Van Mele B. Thermochim Acta 1995;268:121.
- [24] Tatsumiya S, Yokokawa K, Miki K. J Thermal Anal 1997;49:123.
- [25] Lange J, Ekelöf R, St John NA, George GA. ACS Symp Ser 1999; in press.
- [26] Mijovic J, Andjelic S. Macromolecules 1995;28:2787.
- [27] Muller R, Gérard E, Dugand P, Rempp, Gnanou Y. Macromolecules 1991;24:1321.
- [28] Ferry JD. Viscoelastic properties of polymers, New York: Wiley, 1980.
- [29] Hagen R, Salmen L, Lavebratt H, Stenberg B. Polym Testing 1994;13:113.
- [30] Chartoff RP. In: Turi EA, editor. Thermoplastic polymers in thermal characterization of polymeric materials, 2. San Diego: Academic Press, 1997.
- [31] Billmeyer FW. Textbook of polymer science, New York: Wiley, 1984.
- [32] Bair HE. Glass transition measurements by DSC. In: Seyler RJ, editor. Assignment of glass transition, ASTM STP 1249, Philadelphia: American Society for Testing Materials, 1994. p. 50.
- [33] Ward IM, Hadley DW. An introduction to mechanical properties of solid polymers, Chichester, UK: Wiley, 1993.
- [34] Hale A, Macosco CW, Bair HE. Macromolecules 1991;24:2610.